Positioning system for an electric autonomous vehicle based on the fusion of Multi-GNSS RTK and Odometry by using an Extented Kalman Filter

Miguel Tradacete Á.[1], Álvaro Sáez[1], Juan Felipe Arango Vargas[1], Carlos Gómez Huélamo[1], Rafael Barea[1], and María Elena López Guillén[1]

University of Alcalá (UAH), Department of Electronics, Alcal de Henares, Madrid, Spain
tradacete.miguel@gmail.com, alvaro.saezc@edu.uah.es, juanfelipe.arango@edu.uah.es, carlos.gomezh@edu.uah.es, rafael.barea@uah.es, elena@depeca.uah.es,
WWW home page: https://www.robesafe.com/

Abstract. This paper presents a global positioning system for an autonomous electric vehicle based on a Real-Time Kinematic Global Navigation Satellite System (RTK- GNSS), and an incremental-encoder odometry system. Both elements are fused to a single system by an Extended Kalman Filter (EKF), reaching centimeter accuracy. Some varied experiments have been carried out in a real urban environment to compare the performance of this positioning architectures separately and fused together. The achieved aim was to provide autonomous vehicles with centimeter precision on geolocalization to navigate through a real lane net.

Keywords: autonomous vehicle, positioning, odometry, multi-GNSS, Kalman Filter

1 Introduction

Vehicle positioning and tracking have numerous applications in general transport-related studies including vehicle navigation, fleet monitoring, traffic congestion etc. In the last decade, many works have been focused in studying driving behaviour through examining the vehicle movement trajectory using GNSS signals, mostly GPS [1] [2] [3]. These methods have been able to provide both geolocalization and time information to a receiver employing multiple satellite signals while they stay fast, accurate, and cost-efficient. However, their performance has a strong dependence on several system factors such as the number of visible satellites, their positions or the capability of the GPS receiver. In addition, the signal trips through the layers of the atmosphere, and some other sources contribute to inaccuracies and errors in the GPS signals by the time they reach a receiver. Thus, the accuracy provided by this methods is low (usually between 1 and 10 meters), they need a considerable time (over 30 seconds) to provide the

first position measurement and they do not guarantee a robust service in several situations such as environments with poor signal conditions.

The development of Intelligent Vehicles (IVs) has specially grown during the last years. These systems aim to solve complex issues with specially demanding accuracy requirements (usually decimeter precision) like autonomous driving applications where tasks such as lane maintenance analysis demand centimeter precision [4]. Furthermore, autonomous vehicles also require robust solutions with low latencies and high time availability so standalone GNSS techniques are not adequate for them.

Various solutions are proposed to achieve a better service quality: to deal with the accuracy problem Differential GPS (DGPS) is used to obtain an accuracy enhancement using data from a reference station [5] [6] and the more complex Real-time Kinematic (RTK) positioning solution, which uses carrier phase information, has attracted much interest in applications with strict precision requirements due to its centimeter-level accuracy [7]. To approach the robustness issue Multi-GNSS (multiple Global Navigation Satellite Systems) techniques are being widely-used, boosted by the appearance of alternative GNSSs based on different satellite constellations like Russian (GLONASS), European Union (Galileo), Chinese (Beidou) or Japanese (QZSS). Multi-GNSS allows to easily increase the number of tracked satellites to over 10 in good signal conditions and to more than 5 in almost any other situation, even including dense urban areas combining multiple GNSS [4]. Several studies have proven the benefits of these techniques combining GPS and GLONASS [8] [9], GPS and Galileo [10] or even four of the available systems (GPS+Galileo+BeiDou+QZSS) [11].

Nevertheless, even the combination of the previous methods might not be enough to cover autonomous vehicles needs in certain environments such as dense urban or concrete places like tunnels. To face this challenging situations, GNSS data needs to be fused with local sensors information when the measurement's quality is degraded. In [12] RTK-DGPS was fused with speed vehicle sensors and steering-wheel position measurements to improve vehicle tracking. Other works like [13] used an Extended Kalman Filter to integrate DGPS with some vehicle sensors like an inertial navigation system (INS) through a kinematic model in order to achieve enough accuracy to enable vehicle cooperative collision warning without the use of ranging sensors.

This paper presents a robust real-time positioning system for autonomous vehicles that reaches centimeter precision. The system uses a GNSS receiver and an incremental-encoder odometry, integrated by an Extended Kalman Filter which leverages quality of the received satellite measurements. As well as, odometry system is calibrated through an automatic process applying a least square adjustment of the position error of a variety of routes. Experiments presented in Section 4 show that our system is able to keep the vehicle in the middle of the lane nets even in regions without available differential corrections. Furthermore, the system is complemented with a reactive navigation module based on vision and Lidar that slightly relaxes the positioning requirements.

This paper is organized as follows: section 2 presents the system's structure together with an analysis of the main modules that compose it and their corresponding standalone performances. Section 3 analyzes the integration of both modules using the Extended Kalman Filter and the following section 4 exposes the results of the performed experiments to test the final system with different configurations. Last section 5 presents the final conclusions and future work lines.

2   System Architecture

The positioning system is integrated in an open-source electric vehicle (TABBY EVO Vehicle 4 seats version) modified and automatized by the University of Alcalá. The system's architecture includes a Real-Time Kinematic Multi-Global Navigation Satellite System based on both GPS and GLONASS with a local base station that broadcasts differential corrections, a GPRS modem, and an incremental-encoder odometry system. Its sensor equipment is composed of a GNSS receiver, a Choke-Ring Antenna for the local base station, and two Kübler 3700 incremental encoders for odometry. All these modules are fused in Robotic Operating System (ROS) using an Extended Kalman Filter. Figure 1 shows the general diagram of the system.
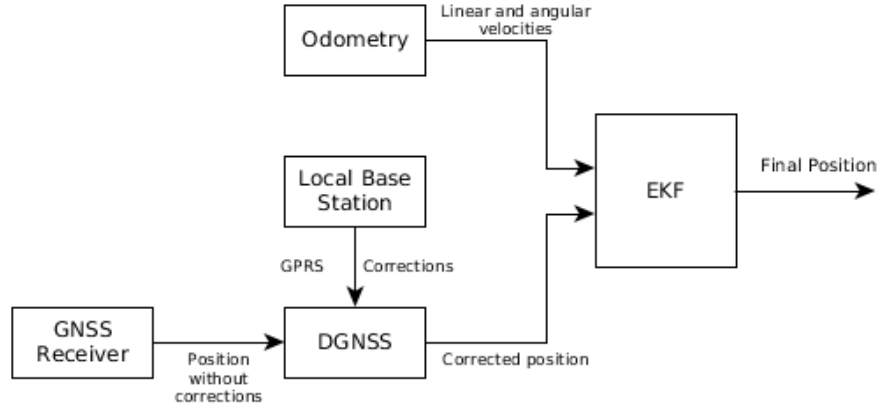
Fig. 1. System Architecture Diagram

GNSS receiver is set on top of the vehicle to obtain maximum coverage, and Choke-Ring Antenna for a base station is set on the Polytechnic School building's roof. The odometry encoders are assembled in both rear-wheel shafts by 3D-printed pieces. ROS runs on two embedded GPUs looking for the benefits of modularity. These GPUs are a Nvidia Jetson TX2, and a Raspberry Pi 3

for odometry processing. Figure 2 displays the entire vehicle, and Figure 3(a) (where Lidar is shown as part of reactive navigation system) and Figure 3(b) show GNSS receiver and odometry encoder details.

Fig. 2. General view of the TABY EVO-OSVehicle

(a) GPS and Lidar   (b) Incremental encoder

Fig. 3. Vehicle sensor equipment

2.1   Multi-GNSS

The main module of the localization system consists of a multi-constellation system (multi-GNSS) with RTK positioning solution. In addition, it also includes

two elements: a differential Hiper Pro GPS+ receiver configured as rover, and a local base station to generate differential corrections.

The rover is able to obtain data from both GLONASS and GPS to provide a more robust solution than a standard GPS by increasing the number of visible satellites. It provides positioning information at 10 Hz as autonomous vehicles demand real-time information. Furthermore, it uses differential corrections to improve the achieved accuracy.

The Standard National Geographic Institute of Spain (IGN) public reference station's frequency is usually below 1 Hz which is inadequate for kinematic applications. In addition, the published data only allows positioning sub-meter level accuracies when the rover is within a short distance from the station. To achieve the needed requirements a local base station was deployed on the Polytechnic School building's roof.

The local base station uses a Choke-Ring Antenna, specifically chosen to deal with multipath. The Antenna is connected to a second Hiper Pro GPS + receiver which generates the differential corrections. Corrections are generated at 10 Hz, published over the Internet using standard Open Source software, and then acquired by the car using a GPRS modem linked via radio.

The GNSS module (base station + rover) was tested separately to evaluate the accuracy it was able to provide. In the first trial, the receiver was tested on standalone mode without adding corrections. To perform the trial an hour of data was recorded on another base station with a known position. The results were then compared with the real station position. Figure 4 shows the results of the experiment. The first graphic, figure 4(a), represents the deviation of the measurements from the real antenna position in meters. The second figure 4(b) represents the RMS error of the measurements (m) as a function of the GPS time.
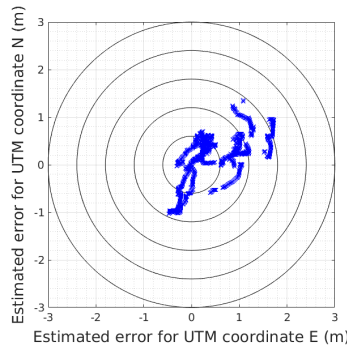
(a) Estimated error for UTM coordinates (m)
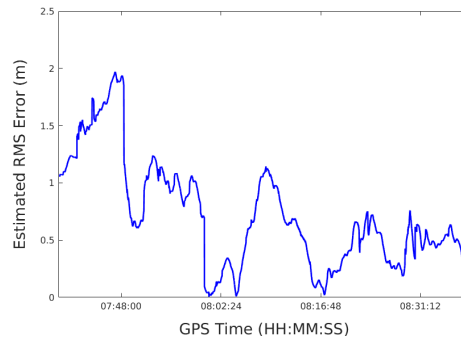
(b) RMS error for estimated position (m)

Fig. 4. GPS+GLONASS performance for standalone receiver

The presented results clearly show that standalone system is not enough for autonomous vehicle applications. With a mean measurement value of 71 cm, the graphs expose the system only provides sub-meter accuracy 72% of the time and for 95% it can only ensure an accuracy of 1.7 meters. Besides, the tested system clearly shows a considerable lack of repeatability when it is analyzed from one day to another.

In a second trial, differential corrections were added to the receiver and the first test was repeated the same day with similar conditions. Another hour of data was recorded after the ambiguity resolution process, in the receiver, and was completed in order to achieve the best accuracy with the Fixed-RTK solution.

(a) Estimated error for UTM coordinates (m)

(b) RMS error for estimated position (m)
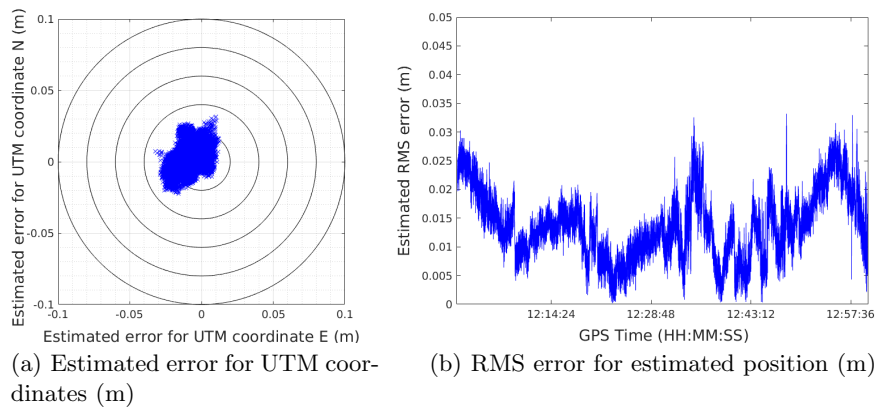
Fig. 5. GPS+GLONASS performance for differential receiver with Fixed-RTK

Figure 5 shows the enhancement that corrections offer: the mean measurement error value is reduced to 1.3 cm with a max deviation of 3.4 cm. The system guarantees centimeter precision 100% of the time and it becomes repeatable if tested on independent days.

Ambiguity resolution process (required to fix the number of wavelengths between satellites and base station, and therefore it provides the optimum solution) is another important issue in the system's performance. Without a fixed solution the accuracy is clearly downgraded. Achieving a fixed-RTK solution takes a long time and it may even be unreachable due to poor satellite visibility. Figure 6 presents the required time to achieve the optimum solution based on collected data during a period of time of two months in favorable conditions (open sky).

The results in figure 6 show that the mean required time (50%) to achieve convergence is over 9 minutes. Furthermore, about 10% of the measurements needed more than 15 minutes to reach centimeter accuracy even with good satellite signal conditions. The convergence time highlights the need to use complementary systems that improve the main module precision when a Fixed solution is not available.
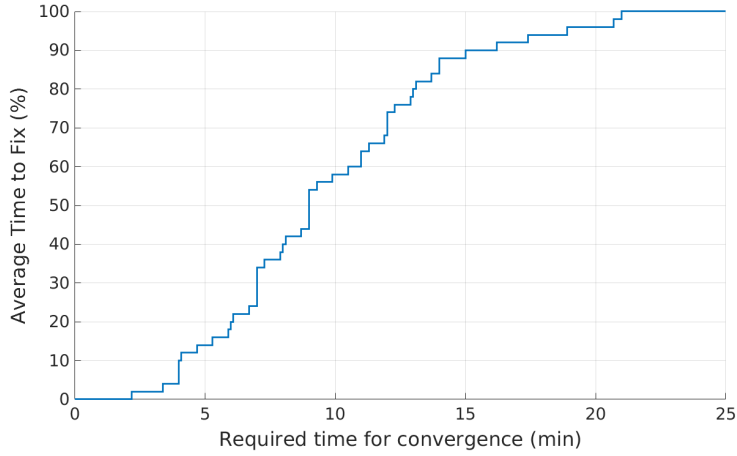
Fig. 6. Convergence time for RTK-Fixed solution.

2.2 Incremental-Encoder Odometry

The implemented odometry system is based on incremental encoders which measure the rear wheels' rotation. Each wheel has its own shaft, which allows the rotation angle of the vehicle to be measured. This odometry system provides the angular and linear velocity of the vehicle to the Extended Kalman Filter.

The relative position and angle are not given to the filter because of cumulative error. Some external causes, such as the irregularity of the road, add error to the measurement each sampling period. The cumulative error is removed by giving instant velocities.

This odometry system is composed of two main modules: a real-time pulse counter, and an algorithm processor. The capturing of pulses is a critical task since missing them implicates losing control of the measurement, and a systematic error. An Olimexino-STM32 is in charge of the counter. Then, the calculations of lineal and angular velocities are performed by a Raspberry Pi 3. This task uses the time between each interaction given by the pulse counter to carry out the calculations of the velocities. These two modules communicate each other through serial-communication protocol.

The calculations of lineal and angular velocities are referenced to the central point between rear wheels, following an Ackerman model [14] as shown in figure 7.

The lineal velocity V_{avrg} is obtained by equation 1 as an average of the two lineal velocities of the wheels, where as V_R is the velocity of the right wheel and V_L is the velocity of the left.

$$V_{avrg} = \frac{V_R + V_L}{2} \tag{1}$$
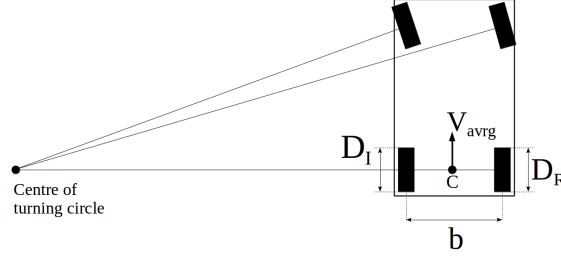
Fig. 7. Vehicle diagram - Ackerman steering geometry

Both independent velocities of each wheel are calculated as

$$V_R = \frac{N_R D_R \pi}{PT} \tag{2}$$

and

$$V_L = \frac{N_L D_L \pi}{PT} \tag{3}$$

where:

N_R number of pulses of the right wheel
N_L number of pulses of the left wheel
D_R diameter of the right wheel
D_L diameter of the left wheel
P encoder resolution (in pulses per revolution of the wheel)
T time between each interaction of calculations

Angular velocity ω_{avrg} is obtained by equation 4 as a lineal derivation of the developed rotation angle θ in each interaction of calculations. This angle is calculated as equation 5.

$$\omega_{avrg} = \frac{\theta}{T} \tag{4}$$

$$\theta = \frac{(N_R D_R - N_L D_L)\pi}{bP} \tag{5}$$

where b is the distance between the rear wheels.

The angle is calculated in this manner as a consequence of the fact the model of the vehicle is based on the Ackerman steering geometry (Figure 7), which implies that every movement is a circular curve. Although this model is only kinematic, it is a appropriate for low velocities [15].

To calibrate the odometry parameters we implemented an automatic process that analyzes different routes to eliminate systematic errors in the calculated position. These errors come from variations in the diameter of the wheels, and the real distance between the wheels. In the performed routes, the position tracks are analyzed, and therefore the calibration process is able to obtain the real odometry parameters D_R, D_L, and b using a least squares adjustment of the position error at the end of the routes.

In order to calibrate the parameters, first, a straight movement has to be analyzed to obtain the real dimensions of the wheels to find the minimum error. Figure 8(a) shows the surface of error in one test, which has a minimum at D_R=560.4 mm and D_L=558 mm. The reasoning behind using a straight route comes from the fact that no turn is made, meaning the distance between wheels b does not interact.

Then, using the calculated dimensions of the wheels, a complex route is analyzed to establish the distance between wheels. The results of the final position error are shown in figure 8(b), with a minimum at b=1404 mm. Finally, figure 9(a) shows the complex route using the nominal value of b (1350 mm), and figure 9(b) shows the same route using the calibrated value of b (1404 mm).
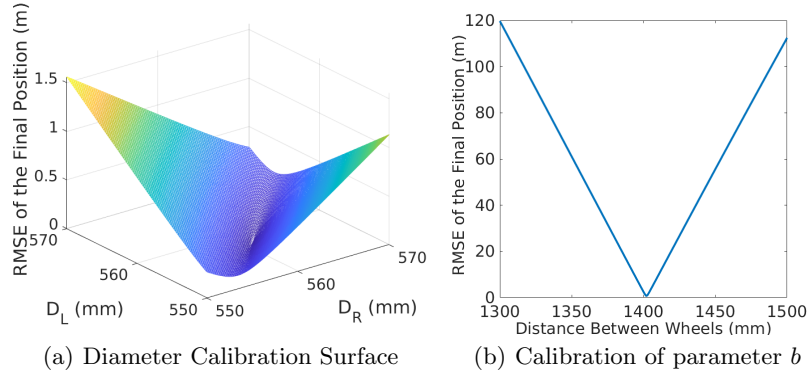

(a) Diameter Calibration Surface   (b) Calibration of parameter b

Fig. 8. Odometry Calibration

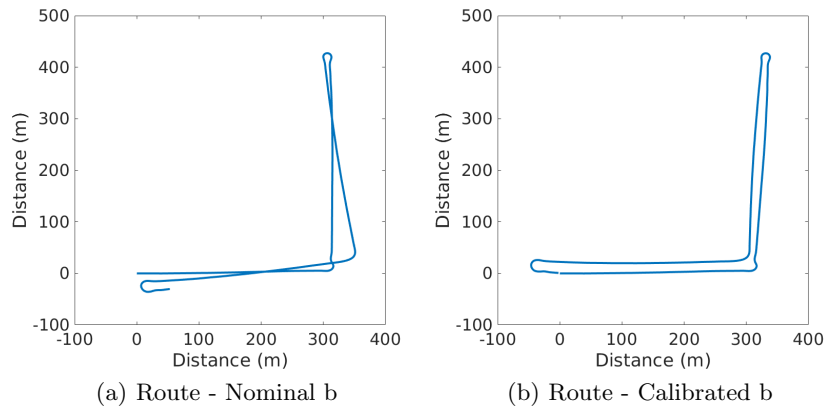(a) Route - Nominal b   (b) Route - Calibrated b

Fig. 9. Complex Route Results

3   Extended Kalman Filter

Standard EKF algorithm and formulation are widely known [16]. To obtain the output of EKF measurement covariance matrices associated with localization sensors are employed. Originally, the raw covariance matrices provided by the sensors were used. However, these matrices only considered certain quality indicators, which were insufficient for the application requirements. For example, the used GNSS receiver only considers some parameters (such as HDOP) but does not leverage the usage of differential corrections, which provide reliable information about measurement accuracy.

Thus, we propose an adaptive filter in accordance with every available quality parameter in order to adapt the output of the filter to the real environment conditions.

3.1   Algorithm

The developed EKF aims to estimate the full 3D pose and velocity of the vehicle over time using the information provided by the previously discussed sensors. The vehicles system state is a six-element vector that comprises the vehicles 3D orientation and velocity. It is calculated as equation 6 where f represents nonlinear state transition function and w_{k-1} is the process noise.

$$x_k = f(x_{k-1}) + w_{k-1} \tag{6}$$

In addition, each employed sensor provides measurements that are modeled as 7:

$$z_k = h(x_k) + v_k \tag{7}$$

where h is a nonlinear state transition sensor function and v_k is the measurements noise which is assumed to be normally distributed.

The prediction stage is described by equations 8 and 9 where a standard 3D kinematic model as product of Newtonian mechanics is used as f. F is the Jacobian of f which is used to project the covariance error P, and finally, Q is the processed noise covariance.

$$\hat{x} = f(x_{k-1}) \tag{8}$$

$$\hat{P}_k = FP_{k-1}P^T + Q \tag{9}$$

The correction stage is carried out through equations 10, 11 and 12. The first one calculates the Kalman gain using the sensors measurement matrix H, the measurement covariance, and the estimated error covariance $\hat{P}_k$. The gain is employed to update the final state vector and the covariance matrix.

$$K = \hat{P}_k H^T (H\hat{P}_k H^T + R)^{-1} \tag{10}$$

$$x_k = \hat{x_k} + K(z - H\hat{x_k}) \tag{11}$$

$$P_k = (I - KH)\hat{P}_k(I - KH)^T + KRK^T \tag{12}$$

The measurement covariance matrices provided by the sensors are adjusted following the GNSS receiver quality indicators: fix quality and Horizontal Dilution of Precision (HDOP). During the first step, the covariance matrices are modified according to fix quality. For a fix quality of 4, the main sensor achieves centimeter precision so matrices are configured to strongly prioritize its information. However, with fix quality of 5, the GNSS receiver has not completed ambiguity resolution process (obtained accuracy is sub-metric), therefore the covariance matrices are adjusted using a linear function dependent on HDOP. Finally, for a fix quality of 1, the GNSS receiver covariance matrix is penalized in benefit of odometry. As it does not provide accurate data, that matrix is adjusted with a linear function as fix quality 5 case.

4   Results

To test the localization system, an area around the UAH campus in Madrid was chosen with approximately 4 km radius distance to the differential corrections base-station, enabling high quality corrections. The test route presented a length of about 5,5 km with both two lane and four lane roads involving challenging tasks for autonomous vehicles such as pedestrian crossings, roundabouts, and stop and give way signs. Additionally, the route has been performed between 20 to 30 kilometers per hour, including defiant conditions for the GNSS signals (trees, high buildings, street signing, electrical lines, etc).

Below we present results of a sample of stretches in the tested routes, showing different configurations and the performance of the system dealing with real-life, challenging situations. In all the figures, the blue trail is the route determined by the GNSS receiver, the yellow one is the path determined by odometry, and the red one is the EKF output.

Figure 10 presents the data collected by sensors along the main section of the route. GNSS receiver achieved the RTK Fix solution during most of the path, but corrections were lost several times due to multipath. The exposed odometry data did not include a calibration process, as it can clearly been observed, but even without the adjustment the output of the system still acts robustly, even under unfavorable conditions. Figure 11 shows the adaptive EKF output for the previous route.

Figure 12 presents different details of the sections (output EKF in red and GNSS output in blue dots) where GNSS signals are degraded by multipath faced by three different system configurations. Figure 12(a) demonstrates the performance of the positioning system without the adaptive Kalman. The results clearly show that basic configuration (with sensor raw covariance matrices) strongly depends on the main module performance and fails when GNSS signals are degraded or lost. Figure 12(b) shows the same section for an adaptive Kalman without a RTK solution available. The performance of the system is clearly improved, even in worse GNSS signal conditions, however the system is still not able to maintain the vehicle between lanes. Figure 12(c) presents the
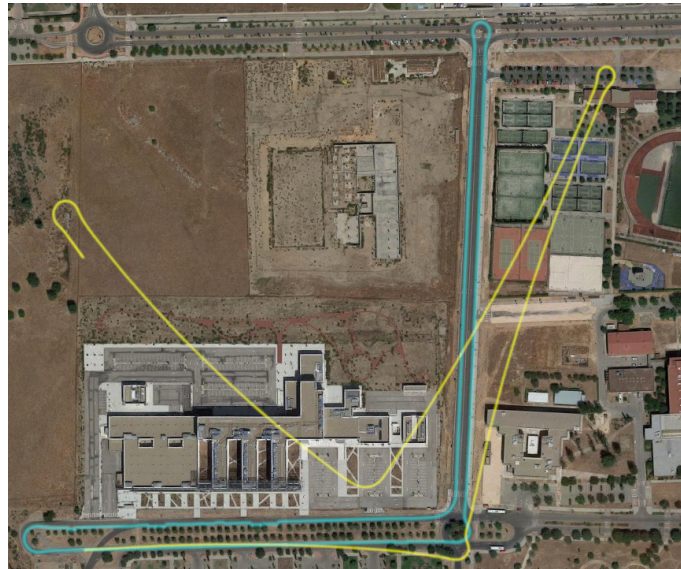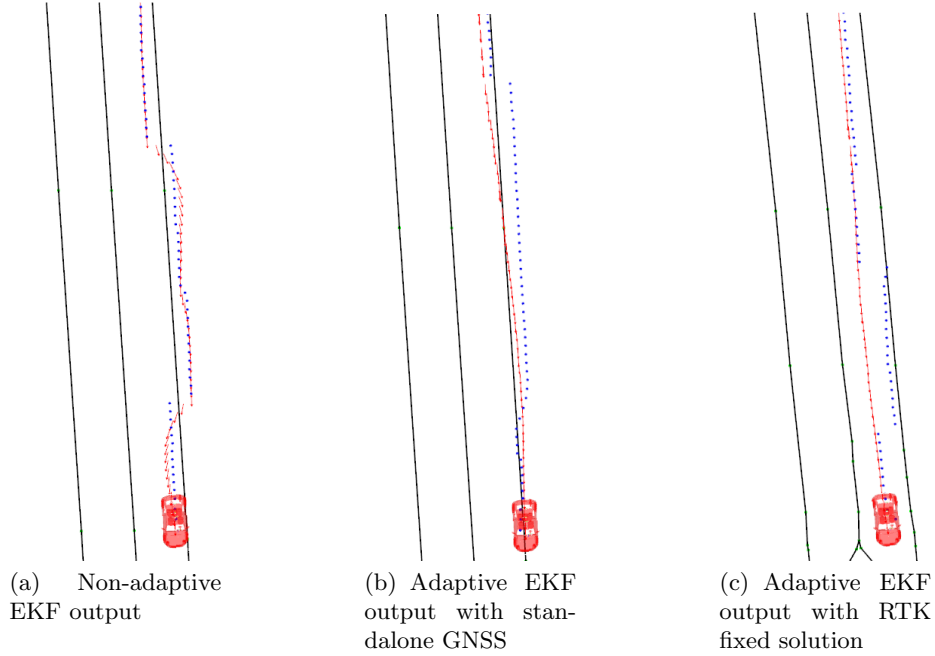
Fig. 10. GNSS standalone fix 1 (blue) and Odometry (yellow)

Fig. 11. Adapted EKF output

performance of the final system with the adaptive Kalman and a RTK positioning solution, which responds correctly to GNSS signal quality degradation.

(a)   Non-adaptive EKF output

(b) Adaptive EKF output with standalone GNSS

(c) Adaptive EKF output with RTK fixed solution

Fig. 12. Adaptive EKF Robustness Example

Figure 13(a) shows the output of the system in a roundabout for a standalone GNSS solution with calibrated odometry and figure 13(b) shows EKF output (red trail) just using odometry information. The performance of the odometry is penalized by sharp turns, so roundabouts are challenging environments for the positioning system if the main module is not able to achieve centimeter accuracy. However, the presented results display the capability of the system to respond properly to this challenging condition.

5   Conclusion

This paper presents an accurate and robust positioning system specifically designed for a fully autonomous vehicle which achieves centimeter precision, even in disadvantageous environments. This positioning system is finally used by a real autonomous vehicle to drive through a lane net, and consequently, in a real urban environment.

The exhibited tests show various potential configurations for the system, which demonstrate the need to use the proposed adaptive EKF in order to

(a) Adaptive EKF output with standalone GNSS

(b) Odometry trial output without EKF
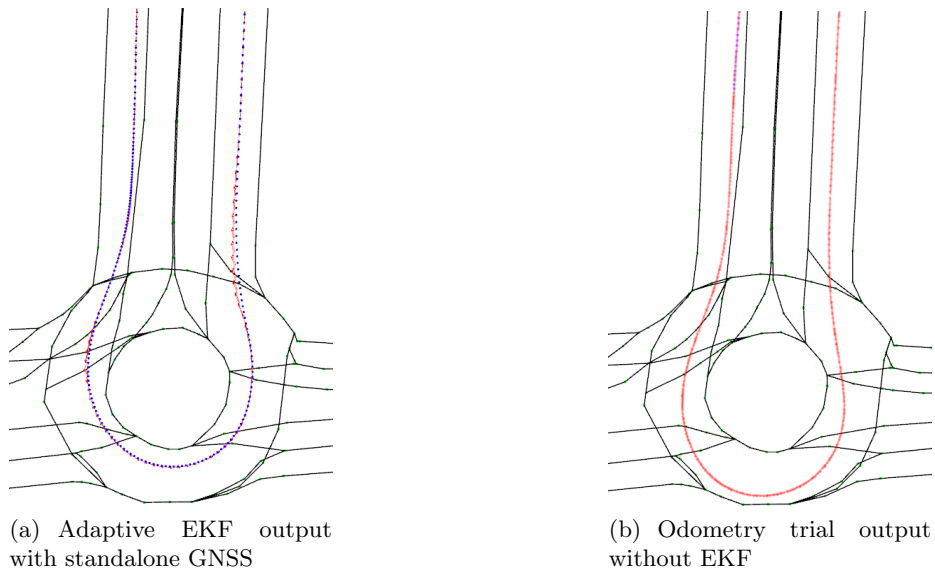
Fig. 13. Improvement over Standalone Odometry Configuration

correctly handle poor sensor performance situations. The importance of using this adaptive EKF lies in the fact that lanes are just a couple meters width. This means, while using standalone GNSS (fix 1 quality) with an non-adaptive EKF, that one meter of error in GNSS receiver positioning could cause a collision.

Future work involves the integration of additional sensors such as a compass and some IMUs to detect possible skids at high velocities, the adaptation of the EKF to more defined, alternative environments such as dense, urban ones, and the readjust of covariance matrix adaptation of all sensors considering the new ones (compass and IMUs). In addition to this, to improve the odometry in real time while driving, the calibration process will be implemented on board using a variety of stretches as test routes when GNSS receiver has Fixed quality.

6   Acknowledgment

References

1. S. Greaves and A. Somers, "Insights on driver behaviour: what can global positioning system (gps) data tell us?," *Publication of: ARRB Transport Research,*

Limited, 2003.

2. H. Ren, T. Xu, and X. Li, "Driving behavior analysis based on trajectory data collected with vehicle-mounted gps receivers," *Wuhan Daxue Xuebao (Xinxi Kexue Ban)/Geomatics and Information Science of Wuhan University*, vol. 39, no. 6, pp. 739–744, 2014.

3. I. Y. Wong, "Using gps and accelerometry to assess older adults' driving behaviours and performance: challenges and future directions," 2013.

4. Q. C. Sun, R. Odolinski, J. C. Xia, J. Foster, T. Falkmer, and H. Lee, "Validating the efficacy of gps tracking vehicle movement for driving behaviour assessment," *Travel Behaviour and Society*, vol. 6, pp. 32–43, 2017.

5. Y. Gao, Z. Li, and J. McLellan, "Carrier phase based regional area differential gps for decimeter-level positioning and navigation," in *Proceedings of the 10th International Technical Meeting of the Satellite Division of The Institute of Navigation (ION GPS 1997)*, pp. 1305–1313, 1997.

6. A. E. Ragheb and A. F. Ragab, "Enhancement of gps single point positioning accuracy using referenced network stations," *World Applied Sciences Journal*, vol. 18, no. 10, pp. 1463–1474, 2012.

7. R. Thitipatanapong, P. Wuttimanop, S. Chantranuwathana, S. Klongnaivai, P. Boonporm, and N. Noomwongs, "Vehicle safety monitoring system with next generation satellite navigation: Part 1 lateral acceleration estimation," tech. rep., SAE Technical Paper, 2015.

8. R. M. Alkan, V. İlçi, I. M. Ozulu, and M. H. Saka, "A comparative study for accuracy assessment of ppp technique using gps and glonass in urban areas," *Measurement*, vol. 69, pp. 1–8, 2015.

9. A. Angrisano, S. Gaglione, and C. Gioia, "Performance assessment of gps/glonass single point positioning in an urban environment," *Acta Geodaetica et Geophysica*, vol. 48, no. 2, pp. 149–161, 2013.

10. S. Verhagen, D. Odijk, P. J. Teunissen, and L. Huisman, "Performance improvement with low-cost multi-gnss receivers," in *Satellite Navigation Technologies and European Workshop on GNSS Signals and Signal Processing (NAVITEC), 2010 5th ESA Workshop on*, pp. 1–8, IEEE, 2010.

11. R. Odolinski, P. J. Teunissen, and D. Odijk, "Combined bds, galileo, qzss and gps single-frequency rtk," *GPS solutions*, vol. 19, no. 1, pp. 151–163, 2015.

12. J. E. Naranjo, C. González, R. García, T. De Pedro, and R. E. Haber, "Power-steering control architecture for automatic driving," *IEEE Transactions on Intelligent Transportation Systems*, vol. 6, no. 4, pp. 406–415, 2005.

13. S. Rezaei and R. Sengupta, "Kalman filter-based integration of dgps and vehicle sensors for localization," *IEEE Transactions on Control Systems Technology*, vol. 15, no. 6, pp. 1080–1088, 2007.

14. A. J. Weinstein and K. L. Moore, "Pose estimation of ackerman steering vehicles for outdoors autonomous navigation," in *Industrial Technology (ICIT), 2010 IEEE International Conference on*, pp. 579–584, IEEE, 2010.

15. S. M. LaValle, *Planning algorithms*. Cambridge university press, 2006.

16. G. Welch and G. Bishop, "An introduction to the kalman filter. university of north carolina, department of computer science," tech. rep., TR 95-041, 1995.